TIDAL TAILS OF STAR CLUSTERS

JOVANA RISOJEVIĆ

Fakulteta za matematiko in fiziko
Univerza v Ljubljani

Inside the Milky Way and other galaxies numerous denser, gravitationally-bound structures can be found, namely star clusters and dwarf galaxies. Tidal tails are extended structures formed by stars escaping from star clusters and dwarf galaxies, due to the influence of the galactic gravitational potential. They can stretch over considerable distances from the progenitors' cores, growing in time until the progenitor is completely dispersed. Beside being impressive structures in their own right, sometimes stretching around the entire galaxy, they can provide useful insights into the distribution of baryonic and dark matter in galaxies. This article explains the formation of tidal tails through the motion of stars in the combined gravitational potentials of the star cluster and the rest of the galaxy. Confirmation of the theory is presented through results from numerical simulations, which are also used to visualize examples that cannot be described analytically. Lastly the article provides a review of observational methods used to detect tidal tails of star clusters.

PLIMSKI REPI ZVEZDNIH KOPIC

Znotraj Rimske ceste in drugih galaksij se nahaja veliko gostejših, gravitacijsko-vezanih struktur, ki se imenujejo zvezdne kopice in pritlikave galaksije. Plimski repi so podolgovate strukture, ki jih ustvarijo zvezde, ki pod vplivom gravitacijskega potenciala galaksije uhajajo iz zvezdnih kopic in pritlikavih galaksij. S časom naraščajo in se lahko raztegnejo do značilnih oddaljenosti od središča kopice oziroma pritlikave galaksije, dokler ta popolnoma ne razpade. Te impresivne strukture, ki se včasih raztezajo okoli celotne galaksije, se lahko uporabijo za preučevanje porazdelitve barionske in temne snovi v galaksijah. Ta članek razlaga nastanek plimskih repov kot posledico gibanja zvezd v skupnem gravitacijskem potencialu zvezdne kopice in preostanka galaksije. Rezultati numeričnih simulacij so predstavljeni za potrditev teorije in vizualizacijo primerov, ki jih ni možno opisati analitično. Končno, članek vsebuje pregled opazovalnih metod, ki se uporabljajo za iskanje plimskih repov zvezdih kopic.

1. Introduction

Star clusters are groups of stars gravitationally bound together. A cluster typically contains from 10^2 to 10^6 stars[1], which have been formed at the same time from a single molecular cloud [2]. In the absence of strong perturbations they are long-lived systems, which are widely used for studying stellar evolution. However, even without external perturbations, clusters lose stars due to internal dynamics and the influence of galactic gravitational field. Escaping stars form two extended structures called tidal tails. Tidal tails are typically extremely difficult to observe, because they are found in densely populated environments. Nevertheless, they have been observed in many clusters, sometimes also showing periodic substructures [3, 4]. Due to observational difficulties, the article mainly deals with tidal tails of clusters in the Milky Way (the Galaxy). Figure 1 shows tidal tails of star cluster Palomar 5, which were the first to be observed [5], due to the cluster's location in scarcely populated Galactic halo. In time, tidal tails spread out along the cluster's orbit and the cluster is eventually fully dispersed.

Tidal tails of star clusters are used to examine gravitational potential of the Galaxy. Learning about the Galaxy as a whole is difficult because we cannot observe it from the outside. This poses a number of problems, for example a large part of the Galaxy is concealed by dust, stellar velocities are always measured relative to the velocity of the Sun, which has its own observational errors, we

[1]Bigger gravitationally bound groups of stars are mainly classified as dwarf galaxies. In addition to stars they usually also contain dark matter so their formation and properties differ from those of star clusters [1].

cannot use gravitational lensing to measure masses, etc. Besides, most of the mass in the Galaxy is in the form of dark matter, which cannot be directly observed. We are therefore limited to observations of kinematic properties of stars and other objects as means of probing the Galactic potential. This could be done by examining orbits of objects around the centre of the Galaxy. But due to the size of the Galaxy, orbital periods of most objects are too long to be observed directly. In the solar neighbourhood the orbital period is (220 ± 30) Myr, so we are practically observing the Galaxy at a fixed point in time [2]. This is where tidal tails can be utilized. Having formed solely due to gravitational interactions, their shape and substructures can provide an insight into the Galactic potential.

Star clusters are not the only objects that form tidal tails, they are also observed in dwarf galaxies that are merging with ours. However, this article will only explore tidal tails of star clusters, which are much more numerous. They are also more suitable for examining matter distribution in the Galaxy, as they are less massive so their potential is often negligible with respect to the Galactic potential and their smaller size makes it easier to locate their centre of mass. In addition, dwarf galaxies are found at larger distances from the Galaxy and are therefore less sensitive to the potential of the inner Galaxy.

In order to use tidal tails for probing the Galactic potential, we need to develop a good understanding of their formation and dynamics. Although we can model large and complicated systems using numerical n-body simulations, this sometimes makes it difficult to discern which effects influence resulting structures the most. Simple analytic descriptions are therefore still useful for obtaining a general idea of the processes involved [3]. This article explores the theory of formation of tidal tails along with numerical and observational methods used to confirm theoretical predictions. Firstly, we provide a theoretical description of the formation of tidal tails. Next, we present results from numerical n-body simulations that confirm the theory. Lastly, we describe observational methods for discovering tidal tails.

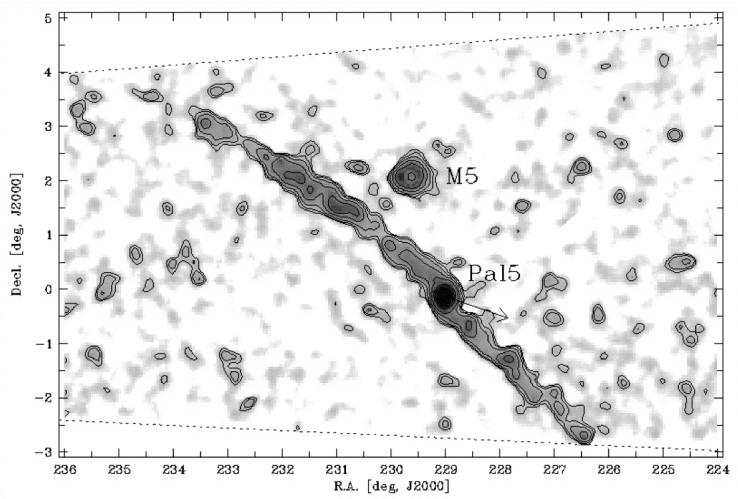

Figure 1. Tidal tails of Palomar 5. The direction of cluster's motion is marked by the arrow pointing away from the cluster. Contours and shades of gray mark the density of stars, varying from 1.5 σ to 5 σ (≈ 0.12 arcmin^{-2}) and higher above the background stellar density of 0.16 arcmin^{-2}. Source [5] © AAS. Reproduced with permission.

2. Formation of tidal tails

Consider a star cluster on an orbit around the centre of the Galaxy. We shall examine how the gravitational potential of the Galaxy influences the motion of stars in the cluster, leading to the formation of tidal tails. Although the Galaxy is comprised of stars, we assume a smooth gravita-

tional field, considering only the forces arising from the overall mass distribution and neglecting the fluctuations from individual stars and other small objects [2]. This is a reasonable assumption, given that the average distance between stars is about 1 pc and the radial extent of the Galaxy is about 10 kpc (1 pc $\approx 3 \times 10^{16}$ m). In addition, significant contribution to the Galactic potential comes from the dark matter, for which the observations suggest a smooth distribution [6]. Since we are dealing only with gravitational forces, the motion of a star is independent of its mass, because the mass of the Galaxy is much larger that that of a star. Therefore, we introduce a unit mass star and write quantities such as momentum and energy per unit mass.

2.1 Motion in a rotating frame of reference

Stars in a cluster move along orbits around the center of the Galaxy, so the gravitational potential they experience is not static. Let's assume a circular orbit with angular velocity $\mathbf{\Omega}$ without imposing any additional symmetries on the potential [2]. We can now choose a non-inertial reference frame that rotates with angular velocity $\mathbf{\Omega}$, called the corotating reference frame, with Cartesian coordinates denoted $\mathbf{x}$. In this frame the potential is static, $\Phi = \Phi(\mathbf{x})$. If we denote the velocity in the corotating frame $\dot{\mathbf{x}}$, then the corresponding velocity in the inertial reference frame is $\dot{\mathbf{x}} + \mathbf{\Omega} \times \mathbf{x}$. The Lagrangian for the motion of a star in a rotating frame of reference is thus

$$\mathcal{L} = \frac{1}{2}|\dot{\mathbf{x}} + \mathbf{\Omega} \times \mathbf{x}|^2 - \Phi(\mathbf{x}).$$

Following the known procedure from classical mechanics we calculate the momentum

$$\mathbf{p} = \frac{\partial \mathcal{L}}{\partial \dot{\mathbf{x}}} = \dot{\mathbf{x}} + \mathbf{\Omega} \times \mathbf{x}.$$

The Hamiltonian is then

$$H_J = \frac{1}{2}p^2 + \Phi - \mathbf{\Omega} \cdot (\mathbf{x} \times \mathbf{p}). \tag{1}$$

Since we have no explicit time dependence, H_J is a conserved quantity, called the Jacobi integral. Its constant value can be written as

$$E_J = \frac{1}{2}|\dot{\mathbf{x}}|^2 + \Phi_{\text{eff}},$$

where we define the effective potential

$$\Phi_{\text{eff}} = \Phi(\mathbf{x}) - \frac{1}{2}|\mathbf{\Omega} \times \mathbf{x}|^2,$$

as the sum of the gravitational and centrifugal potentials. We can find stationary points of Φ_{eff}, called the Lagrange points, by considering $\nabla\Phi_{\text{eff}} = 0$.

For further discussion it is necessary to choose a concrete potential Φ. A star in a cluster is influenced by the other stars in the cluster, so we can write the potential as a sum of the cluster's potential and the potential from the rest of the Galaxy. Therefore, we can adopt the familiar three body problem as a first approximation. We investigate the motion of a unit mass star in the combined gravitational potential of the cluster and the rest of the Galaxy, approximated as point masses m and M, respectively. This is not a realistic description, because point-mass approximations only hold at great distances and in our case the cluster is inside the Galaxy, but it will give us intuitive understanding of the formation of tidal tails. The point masses orbit their mutual center of mass at separation R_0, with angular speed [2]

$$\Omega = \sqrt{\frac{G(M+m)}{R_0^3}},$$

where G is the gravitational constant. The gravitational field is thus static in the reference frame rotating at Ω and centred at the center of mass of the system. We orient the coordinate system such that $\mathbf{\Omega} = (0, 0, \Omega)$ and the point masses are at $\mathbf{x}_m = (MR_0/(M+m), 0, 0)$ and $\mathbf{x}_M = (-mR_0/(M+m), 0, 0)$. The effective potential is then

$$\Phi_{\text{eff}} = -G\left[\frac{M}{|\mathbf{x}-\mathbf{x_M}|} + \frac{m}{|\mathbf{x}-\mathbf{x_m}|} + \frac{M+m}{2R_0^3}(x^2+y^2)\right],$$

where $\mathbf{x} = (x, y, z)$. Contours of constant effective potential in the equatorial plane of the two orbiting masses are shown on the left side of Figure 2. In this case, there are five Lagrange points labelled L_1 to L_5. L_1 to L_3 are saddle points, and L_4 and L_5 are minima points of the effective potential. We can see that the contours, and corresponding surfaces in three dimensions, enclose each of the masses separately at smaller radii while at larger radii they surround both masses. The last surface that surrounds a single body is called its tidal surface. Since it touches the point L_1, we define the radius of the outermost orbit still bound to m as the distance r_J between L_1 and x_m, and refer to it as the Jacobi or tidal radius. We can calculate it by remembering that L_1 is a stationary point of Φ_{eff}

$$0 = \frac{1}{G}\left(\frac{\partial\Phi_{\text{eff}}}{\partial\mathbf{x}}\right)_{(x_m-r_J,0,0)} = \frac{M}{(R_0-r_J)^2} - \frac{m}{r_J^2} - \frac{M+m}{R_0^3}\left(\frac{MR_0}{M+m} - r_J\right).$$

The equation must in general be solved numerically, but if $r_J \ll R_0$ we can obtain an approximate result to first order in r_J/R_0 [2]

$$r_J = \left(\frac{m}{3M}\right)^{1/3} R_0. \tag{2}$$

Although this result was derived in the point-mass case, the general idea still holds for more realistic potentials, such as the Plummer potential (see Appendix A) shown on the right side of Figure 2. The combined field of the cluster and the rest of the Galaxy has two saddle points around the cluster, determining the radii of orbits bound to the cluster and ultimately its size. It is through these points that stars with sufficient energy can escape the cluster forming tidal tails. Points L_3 to L_5 can be ignored because they are sufficiently far away from the cluster. By losing stars the mass of the cluster diminishes thus shrinking the tidal surface until the cluster is fully dispersed [7]. It is worth noting that the only contribution to the cluster's mass is from its stars. Clusters do not contain any gas or dark matter.

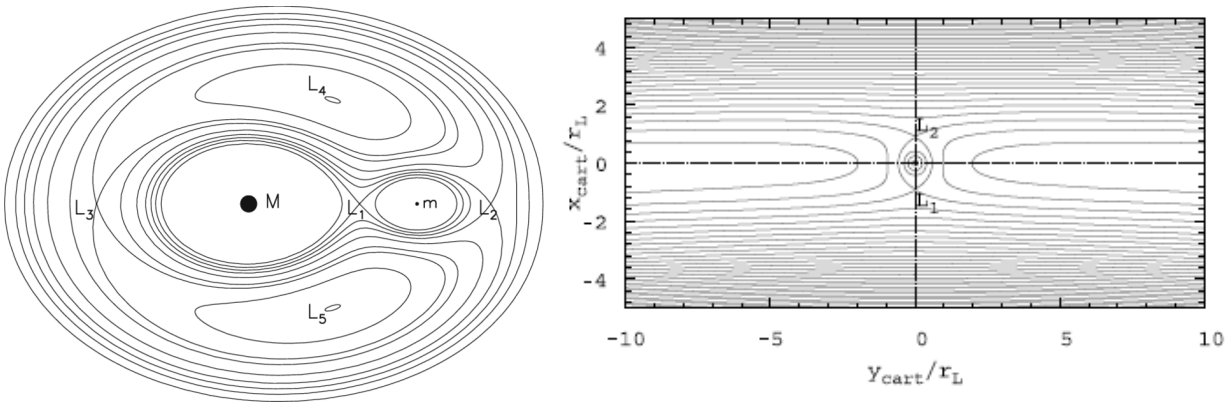

Figure 2. Left: Contours of constant Φ_{eff} in the equatorial plane of the two orbiting masses for the three body problem example. The mass ratio is $m/M = 1/5$. Lagrange points are labelled as L_1 to L_5. Source [8]. Right: Contours of constant Φ_{eff} for a more realistic example of a cluster in the Galaxy's gravitational field. Two saddle points are labelled as L_1 and L_2, r_L is the tidal radius. Source [7].

We should keep in mind that our discussion has so far only included clusters on circular orbits. In the case of eccentric orbits the angular velocity is not constant so we cannot find a reference frame in which Φ is static. Therefore, no analogue of the Jacobi integral exists and we cannot generalize our derivation of the tidal radius to eccentric orbits. However, analogues of Lagrange points still exist so we can intuitively understand that not much changes in the overall picture. The important difference is that the size of the tidal surface changes along the orbit, being smallest at the perigalacticon, the point closest to the centre of the Galaxy, and largest at the apogalacticon, the point farthest away from the centre of the Galaxy. Since equation (2) is a simple analytic expression, we can abuse it to get a crude estimate of the sizes involved. Assuming a cluster of mass $m = 3\,000\ \mathrm{M}_\odot$ and a galaxy of mass $m = 10^{12}\ \mathrm{M}_\odot$, where $\mathrm{M}_\odot$ is the mass of the Sun, on a circular orbit of radius $R_0 = 8.5$ kpc, which is the distance from the Solar System to the Galactic centre, we obtain tidal radius $r_J = 8.5$ pc. For an orbit with eccentricity $\epsilon = 0.25$, which is one of the most eccentric orbits for clusters, keeping the apogalactic distance at 8.5 kpc, the perigalactic distance is 5.1 kpc [9], so the tidal radius at perigalacticon is $r_J = 5.1$ pc. Hence, we expect that clusters on eccentric orbits lose most of their stars close to perigalacticon [2].

2.2 Distant-tide approximation and epicyclic motion

Having discussed the general properties of rotating potentials, we are now interested in the motion of stars within the tidal tails. Using the Hamiltonian from equation (1) we can write down the equations of motion in a rotating potential [2]

$$\dot{\mathbf{p}} = -\frac{\partial H_J}{\partial \mathbf{x}} = -\nabla\Phi - \boldsymbol{\Omega} \times \mathbf{p}$$
$$\dot{\mathbf{x}} = -\frac{\partial H_J}{\partial \mathbf{p}} = \mathbf{p} - \boldsymbol{\Omega} \times \mathbf{x}.$$

Eliminating $\mathbf{p}$ we get

$$\ddot{\mathbf{x}} = -\nabla\Phi - 2\boldsymbol{\Omega} \times \dot{\mathbf{x}} - \boldsymbol{\Omega} \times (\boldsymbol{\Omega} \times \mathbf{x}), \tag{3}$$

where we recognize the Coriolis force $-2\boldsymbol{\Omega} \times \dot{\mathbf{x}}$ and the centrifugal force $-\boldsymbol{\Omega} \times (\boldsymbol{\Omega} \times \mathbf{x})$.

Because we are considering motion of a star in a cluster, we can write the potential as a sum of contributions from the cluster and the rest of the Galaxy, $\Phi = \Phi_c + \Phi_g$. The size of the cluster is typically much smaller than its distance from the centre of the Galaxy, therefore we can expand $\nabla\Phi_g$ around the centre of the mass of the cluster, $\mathbf{x_0}$. The jth component of the gradient is then [2]

$$\frac{\partial \Phi_g}{\partial x_j} = \frac{\partial \Phi_g}{\partial x_j}\Big|_{\mathbf{x_0}} + \sum_k \frac{\partial^2 \Phi_g}{\partial x_j \partial x_k}\Big|_{\mathbf{x_0}} x_k + \ldots \tag{4}$$

Dropping the higher order terms constitutes so-called distant-tide approximation. Now we shall move to a reference frame centred on the cluster (centre of mass system, CMS). Let α be some star in the cluster and m_α its mass. We denote its velocity in the corotating frame $\mathbf{v}'_\alpha$. The acceleration in the CMS can be written as

$$\dot{\mathbf{v}}_\alpha = \dot{\mathbf{v}}'_\alpha - \dot{\mathbf{v}}_{\mathrm{cm}}, \tag{5}$$

where $\dot{\mathbf{v}}_{\mathrm{cm}}$ is the acceleration of the centre of mass

$$\dot{\mathbf{v}}_{\mathrm{cm}} = \frac{1}{\sum_\beta m_\beta} \sum_\beta m_\beta \dot{\mathbf{v}}'_\beta. \tag{6}$$

Substituting equations (3) and (4) into (6) we find that the term $\sum_k \frac{\partial^2 \Phi_g}{\partial x_j \partial x_k}\Big|_{\mathbf{x_0}} x_k$ does not contribute to the centre of mass acceleration, because the centre of mass is at the origin of the new reference

frame so $\sum_\beta m_\beta \mathbf{x}_\beta = 0$. Next substituting into equation (5) we find that the term $\frac{\partial \Phi_g}{\partial x_j}\Big|_{\mathbf{x_0}}$ cancels out, so only the $\sum_k \frac{\partial^2 \Phi_g}{\partial x_j \partial x_k}\Big|_{\mathbf{x_0}} x_k$ term contributes to the motion of a star in the CMS [2]. To evaluate it, we assume an axisymmetric potential Φ_g, which is a reasonable approximation for disk galaxies. We orient the coordinate system so that the x and y coordinates lie in the cluster's plane of motion, x points away from the centre of the Galaxy and y points in the direction of cluster's motion, which is the usual choice in the theory of Galactic dynamics. The angular velocity then points in the z direction $\mathbf{\Omega} = (0, 0, \Omega)$. We introduce cylindrical coordinates (R, Z), where R is the radial coordinate in the cluster's plane of motion, $R = \sqrt{x^2 + y^2}$. The potential is then $\Phi_g = \Phi_g(R, z)$ and the distance to the centre of the Galaxy is denoted R_0. Expressed in cylindrical coordinates, the $\frac{\partial^2 \Phi_g}{\partial x_j \partial x_k}\Big|_{\mathbf{x_0}}$ components in the plane of motion are [10]

$$\begin{aligned}
\frac{\partial^2 \Phi_g}{\partial x^2}\Big|_{\mathbf{x_0}} &= \Phi_g''(R_0), \\
\frac{\partial^2 \Phi_g}{\partial y^2}\Big|_{\mathbf{x_0}} &= \frac{\Phi_g'(R_0)}{R_0}, \\
\frac{\partial^2 \Phi_g}{\partial x \partial y}\Big|_{\mathbf{x_0}} &= \frac{\partial^2 \Phi_g}{\partial y \partial x}\Big|_{x_0} = 0,
\end{aligned}$$

where we have denoted $\frac{\partial \Phi_g}{\partial R} = \Phi_g'$ and $\frac{\partial^2 \Phi_g}{\partial R^2} = \Phi_g''$. Since we are considering circular orbits in axisymmetric potential, $\Phi_g' = R\Omega^2$ and the motion in the orbital plane is decoupled from the motion in z direction. Tying everything together, we obtain the equations of motion in the orbital plane from equation (3)

$$\begin{aligned}
\ddot{x} &= 2\Omega\dot{y} + \left[\Omega^2 - \Phi_g''(R_0)\right] x - \frac{\partial \Phi_c}{\partial x}, \\
\ddot{y} &= -2\Omega\dot{x} + \left[\Omega^2 - \frac{\Phi_g'(R_0)}{R_0}\right] y - \frac{\partial \Phi_c}{\partial y}.
\end{aligned}$$

Using $\Phi_g'(R_0) = R_0\Omega^2$, we can cancel out the terms in the square brackets of equation $\ddot{y}$. It is common to write the term $\Omega^2 - \Phi_g''(R_0)$ as $\kappa^2 - 4\Omega^2$, where κ is called the epicyclic frequency [3]. The final equations of motion are then

$$\begin{aligned}
\ddot{x} - 2\Omega\dot{y} + \left(\kappa^2 - 4\Omega^2\right) x &= -\frac{\partial \Phi_c}{\partial x}, \\
\ddot{y} + 2\Omega\dot{x} &= -\frac{\partial \Phi_c}{\partial y}.
\end{aligned} \tag{7}$$

Once the star has left the cluster, the influence of its potential rapidly diminishes, so we can set the right-hand side of equation (7) to zero. Most of the escaping stars have energies only slightly higher then the value of effective potential at the Lagrange point, because if there were many stars with high energies the cluster would disperse quickly and we couldn't observe it as a single object. Besides that, stars in the cluster interact and the relaxation time of the cluster is much shorter then its lifetime, so it is unlikely that we get many energetic stars. Assuming therefore that the star leaves through the Lagrange point located at $(x_L, 0, 0)$ at time $t = 0$ with zero initial velocity, the solution for equation (7) can be written as [3]

$$\begin{aligned}
x &= \frac{4\Omega^2}{\kappa^2} x_L + \left(1 - \frac{4\Omega^2}{\kappa^2}\right) x_L \cos(\kappa t), \\
y &= -\frac{2\Omega}{\kappa}\left(1 - \frac{4\Omega^2}{\kappa^2}\right) x_L (\sin \kappa t - \kappa t).
\end{aligned}$$

Similarly, we can find the solution for the stars leaving through the Lagrange point $(-x_L, 0, 0)$. The solutions describe the motion of stars in the tidal tails in the CMS, called the epicyclic motion. The motion is depicted in Figure 3. Stars leaving through $(x_L, 0, 0)$ orbit the centre of the Galaxy somewhat closer then the cluster's centre of mass and form the so-called leading arm of the tidal tail while the stars leaving through $(-x_L, 0, 0)$ orbit somewhat further and form the trailing arm. As we can see from Figure 3, after leaving the Lagrange point, the star moves on an oscillatory path

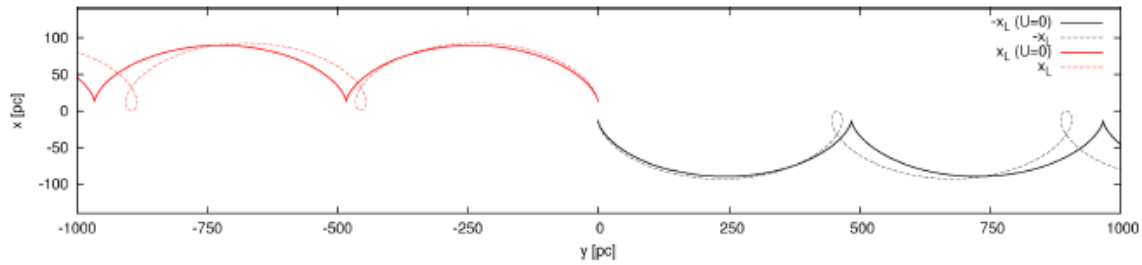

Figure 3. Epicyclic motion of stars in tidal tails. Solid lines correspond to solutions of equation (7) with $\Phi_c = 0$, dashed lines correspond to the solutions with point-mass approximation for the cluster potential. Mass of the cluster used the for plot is $M = 1\,000\ \mathrm{M}_\odot$, where $M_\odot = 2 \times 10^{30}$ kg is the mass of the Sun, and the distance to the Lagrange point is $x_L = 12.9$ pc, pc $\approx 3 \times 10^{16}$m. Source [3].

and comes to rest again at the cusp of the orbit. This happens at time

$$t = t_C = \frac{2\pi}{\kappa}.$$

The y coordinate is then

$$y_C = \pm \frac{4\pi\Omega}{\kappa} \left(1 - \frac{4\Omega^2}{\kappa^2}\right) x_L.$$

Because the y-component of velocity is zero at $y = y_C$, we expect stars to clump at this point. These periodic clumps along tidal tails are called epicyclic overdensities and are formed when the first stars reach $y = y_C$. As the cluster loses mass x_L decreases and so does y_C, so the overdensities move closer to the cluster as it dissolves [3]. In the next section, we will present results from numerical modelling that confirm this behaviour.

Throughout this analysis we have treated the stars leaving the cluster as single stars. In reality many stars are found in binary systems, where two stars orbit a common centre of mass, which affects their kinematics. However, since our analysis is already simplified and binary systems are stable, in case of a binary system leaving the cluster it suffices to approximate orbits of both stars with the orbit of their centre of mass. A more precise calculation, needed for comparing theoretical predictions with observations, is achieved through numerical modelling, where kinematics of individual stars in a binary system can be tracked.

3. Numerical modelling

Results obtained from a somewhat simplified theory in the previous section can be checked through numerical n-body simulations. After setting up initial states for the stars in the cluster, their motion is followed through time. By taking snapshots at different moments in time, we can check whether the evolution of the cluster is consistent with our theoretical predictions. Initial conditions for the stars in the cluster are usually chosen such that they represent a virialized system. This means that the system obeys the virial theorem, $2T = -U$, where T and U are total kinetic and potential energies of the system, respectively. The condition is typical for spherical, gravitationally-bound systems in equilibrium.

We have so far only considered clusters on circular orbits, so let us first examine a simulation of such an example from [7]. The simulated cluster initially has mass $m = 10^4$ M$_\odot$ and consists of 40 404 stars. It is set on a circular orbit of radius $R_0 = 8.5$ kpc in an axisymmetric galactic potential described by the Plummer-Kuzmin model (see Appendix A). The initial tidal radius of the cluster is $r_L = 30$ pc and epicyclic frequency normalized to angular velocity is $\kappa/\Omega = 1.372$. Results of the simulation at two different times are shown in Figure 4. We can see that the stars have formed leading and trailing arms of the tidal tail emerging from the tidal surface. Epicyclic overdensities are clearly visible and their positions move closer to the cluster at later times, as the tidal radius shrinks. Therefore, the positions and local densities of stars are consistent with our theoretical predictions.

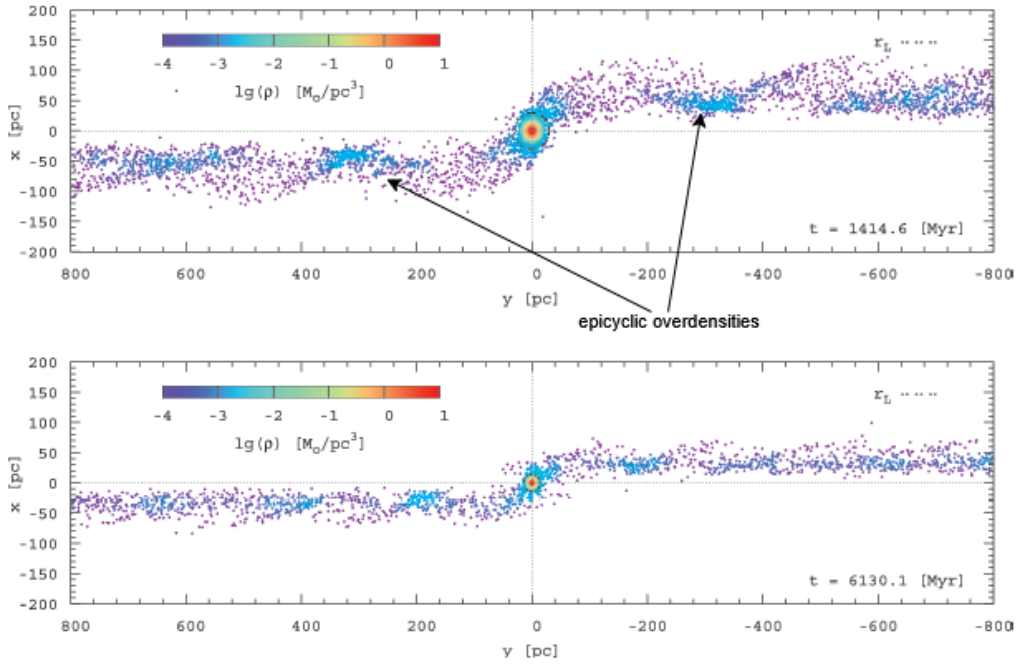

Figure 4. Results of n-body simulations at two different times for a cluster on circular orbit. The colour scheme represents the local star density. The dotted circle marks the tidal radius. Source [7].

Having confirmed predictions from the theory, we can now utilize n-body simulations to visualize tidal tails in the case of eccentric cluster orbits, which cannot be described analytically. As discussed in section 2.1, we expect the shape of tidal tails to vary between cluster's orbital phases. Since the tidal radius is smallest at the perigalacticon, most of the cluster's stars become unbound during pericentre passages. However, escaping stars typically have low velocities, so they can stay close to the cluster even if they are outside of the current tidal radius. As the cluster moves, the tidal radius expands, so the unbound stars can get recaptured, with slightly higher energies then before. This increase in energy will eventually cause the stars to escape again, but this could happen considerable amount of time after the pericentre passage. Therefore, not all stars that are outside of the tidal radius at a given time are lost to the cluster and tidal radius is no longer such a good measure of cluster's gravitational influence. Following an example given in [9], we define eccentricity of cluster's orbit as $\epsilon = (R_{\rm apo} - R_{\rm peri})/(R_{\rm apo} + R_{\rm peri})$, where $R_{\rm apo}$ is cluster's apogalactic distance and $R_{\rm peri}$ its perigalactic distance. The cluster initially consists of 65 536 stars and has a mass of about 20 000 M$_\odot$. Eccentricity of the orbit is $\epsilon = 0.25$, with $R_{\rm apo} = 8.5$ kpc and $R_{\rm peri} = 5.1$ kpc. Snapshots from the simulation at three different orbital phases are shown in Figure 5. We can see that the tidal tails retain the overall epicyclic structure with visible overdensities, but their shape and density change during the orbit. The epicyclic loops are most prominent at the apogalacticon, where they

are similar to the case of circular orbits but squeezed together. Between apo- and perigalacticon the loops get stretched, reaching maximum length at the perigalactiocon. The epicyclic structure is least visible at this point and overdensities are further away from the cluster's core. Between peri- and apogalacticon the loops become squeezed together again, eventually forming the structure seen at the apogalacticon again. At first glance this seems to be in contradiction with our theoretical predictions. Since the tidal radius is smallest at perigalacticon and the distance to overdensities increases with the tidal radius, we would expect the overdensities to be closer to the cluster at perigalacticon. However, due to the non-linearly accelerated reference frame, the opposite happens. From apo- to perigalacticon the cluster and its tidal tails get accelerated and stretched, resulting in more distant overdensities at perigalacticon. In the other half of the orbit the tails get compressed as the system is decelerated, making the epicyclic structure more apparent at the apogalacticon.

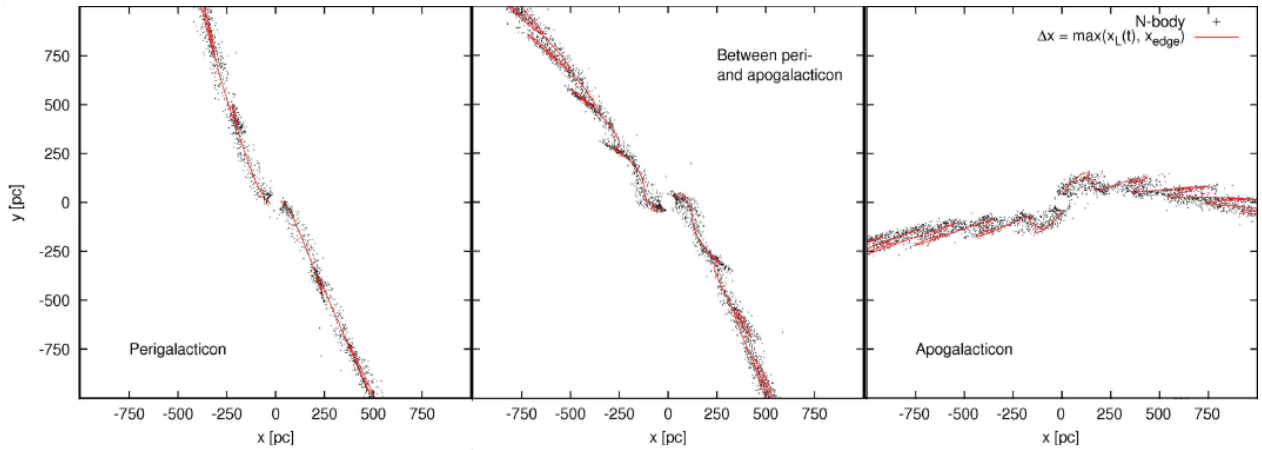

Figure 5. Results of a simulation at three different orbital phases for a cluster with orbital eccentricity $\epsilon = 0.25$. At the time of the snapshots the cluster has lost 5 000 $M_\odot$ of its mass. Stars within a radius of 40 pc are omitted for clarity. Black dots correspond to n-body simulations, while red lines represent the trajectories of stars in the galactic potential initialized at $\Delta x = \max(x_L(t), x_{\rm edge})$ with zero velocity, where $x_{\rm edge}$ marks the radius beyond which unbound stars cannot be recaptured. Source [9].

4. Observations

Observing tidal tails of star clusters poses some difficulties, because in the same part of the sky where we find stars belonging to the tidal tails, we also find other stars which have no connection to the cluster. These are called field stars and they need to be filtered out from observations when studying tidal tails. The presence of field stars makes it impossible to detect stars in tidal tails solely based on their location, so we need to find other properties that distinguish them from their surroundings.

First observational confirmation of tidal tails of star clusters was made in 2001. Two structures were found emerging from the cluster Palomar 5, forming the leading and trailing arm of the tidal tail. Within the tail it was possible to discern two stellar overdensities, one in each arm, located symmetrically at 320 pc from the cluster's core (see Figure 1). Stars in the tails were detected using photometry, i.e. measurements of the colours and luminosities of stars [11]. Data obtained from observations of star clusters in general shows that there exists a relationship between these quantities specific for a given cluster. Because the stars in the tidal tails were once part of the cluster, we can utilize this relationship to separate them from field stars. The method proved useful for Palomar 5 and few other tidal tails of clusters and dwarf galaxies in otherwise scarcely populated Galactic halo.

This was a primary way of detecting tidal tails up to 2014. Although the method was successful,

it was limited to observations of large clusters with many bright stars, since smaller clusters and fainter stars would have required the use of much better instruments. Another way of discerning stars in tidal tails is through their kinematic properties. This was made possible by the Gaia mission. During the mission, from December 2013 to January 2025, Gaia spacecraft observed 1.8 billion stars and other objects, providing, among other data, most precise measurements of positions and velocities of the Milky Way stars yet. Knowing that stars in tidal tails share similar orbits, these measurements enabled us to search for tidal tails as overdensites in the position-velocity or energy-momentum phase-space. The method can be used even for nearby clusters, whose tidal tails appear broad in the sky projection. Thus Gaia's data increased the number of detected tidal tails by an order of magnitude, from ≈ 10 to ≈ 100 [12].

Detection of tidal tails through kinematics is still the main method used today. However, despite the large number of found tidal tails, searching for overdensities in phase-space is mostly effective for clusters in the Galactic halo. Clusters in the Galactic disk are typically smaller and found in more densely populated environments, so their tidal tails do not form significant overdensities. Therefore, another method must be used for detecting them. By simulating dissolution of a cluster it is possible to obtain a probability distribution for cluster members in the phase-space. Comparing this to the Gaia models of Galactic stellar populations yields membership probabilities for individual stars. This way, we can detect stars in tidal tails, even at large distances from clusters' cores, without relying on overdensities in phase-space [4]. Figure 6 shows tidal tails of cluster Alessi 3, which were detected using described method.

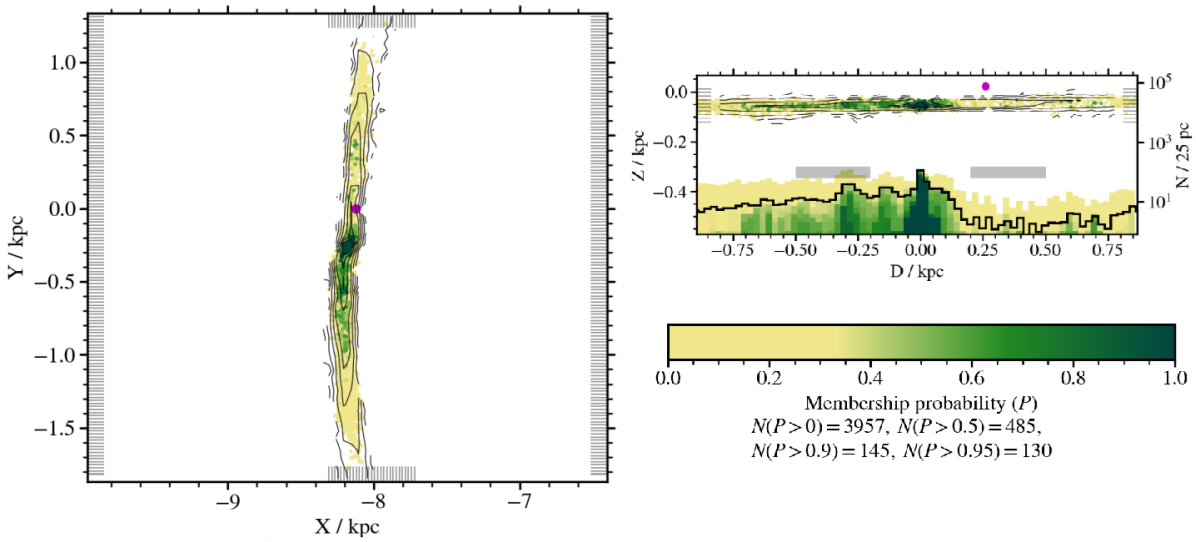

Figure 6. Tidal tails of cluster named Alessi 3, detected using a probabilistic method. Tails are displayed in Galactocentic (XYZ) coordinate system, where the Galactic centre is at the origin and Sun is located at (-8.122, 0.0, 0.0208) kpc. Purple dot marks the position of the Sun. Left plot shows the tails in the XY plane, while the right plot shows the view in the Galactic plane. D is the dimension along the cluster's major axis. The histogram at the bottom of the right plot shows star count in 25 pc bins. Source [4].

5. Conclusions

Having formed through gravitational interactions, tidal tails of star clusters are excellent probes of the Galactic gravitational potential. Development of n-body simulations enabled us to study their evolution in a variety of complex scenarios. Using observational data from the Gaia mission, we can compare simulation results to shapes of real tidal tails and thus constrain the matter distribution in the Galaxy. Perturbations in tidal tails are used to detect possible substructures in the Galactic

dark matter halo, which are predicted by the ΛCDM cosmological model [6, 12]. At the same time, tidal tails of dwarf galaxies, which are formed similarly to tidal tails of star clusters, are used to constrain the overall shape of the dark matter halo [12]. In the article we described how tidal tails of star clusters are formed due to the influence of Galactic potential on the motion of stars in the cluster. We derived analytic expressions for the motion of stars in tidal tails for the simple case of a cluster on a circular orbit. These results proved to be enough to explain the formation of substructures within the tidal tails. We presented numerical n-body simulation data which confirmed the theoretical predictions and provided insights into the formation and evolution of tidal tails in more complicated cases of eccentric cluster orbits, which couldn't be described analytically. Lastly we reviewed observational methods for detecting tidal tails and addressed the main difficulties of this process. Precisely identifying the shapes of tidal tails in the Galaxy is crucial for understanding the way they formed. It is therefore expected that new methods for detecting members of tidal tails will be developed in the future. This data could then be used to further constrain the Galactic potential and provide insights into the matter distribution and formation of the Galaxy.

Acknowledgements

I would like to thank my advisor, Dr. Janez Kos, for his support and guidance.

REFERENCES

[1] G. Gilmore, M.I. Wilkinson, R.F.G. Wyse, J.T. Kleyna, A. Koch, N.W. Evans and E.K. Grebel, *The Observed Properties of Dark Matter on Small Spatial Scales*, The Astrophysical Journal **663** (2007), 948–959

[2] J. Binney and S. Tremaine, *Galactic Dynamics*, Princeton University Press, 2008

[3] A.H.W. Küpper, A. Macleod, and D.C. Heggie, *On the structure of tidal tails*, Monthly Notices of the Royal Astronomical Society **387** (2008), 1248–1252

[4] J. Kos, *Tidal tails of open clusters*, Astronomy & Astrophysics **691** (2024), A28

[5] M. Odenkirchen, E.K. Grebel, W. Dehnen, H. Rix, B. Yanny, H.J. Newberg, C.M. Rockosi, D. Martinez-Delgado, J. Brinkmann, and J.R. Pier, *The Extended Tails of Palomar 5: A 10° Arc of Globular ClusterTidal Debris*, The Astronomical Journal **126** (2003), 2385

[6] A. Mastrobuono-Battisti, P. Di Matteo, M. Montuori and M. Haywood, *Clumpy streams in a smooth dark halo: the case of Palomar 5*, Astronomy & Astrophysics **546** (2012), L7

[7] A. Just, P. Berczik, M.I. Petrov and A. Ernst, *Quantitative analysis of clumps in the tidal tails of star clusters*, Monthly Notices of the Royal Astronomical Society **392** (2009), 969–981

[8] R.J. Klement, *Halo streams in the solar neighborhood*, The Astronomy and Astrophysics Review **18** (2010), 567–594

[9] A.H.W. Küpper, R.R. Lane and D.C. Heggie, *More on the structure of tidal tails*, Monthly Notices of the Royal Astronomical Society **420** (2012), 2700–2714

[10] A. De Biasi, L. Secco, M. Masi, and S. Casotto, *Galactic planar tides on the comets of Oort Cloud and analogs in different reference systems. I.*, Astronomy & Astrophysics **574** (2015), A98

[11] M. Odenkirchen, E.K. Grebel, C.M. Rockosi, W. Dehnen, R. Ibata, H.W. Rix, A. Stolte, C. Wolf, J.E. Anderson, Jr, N.A.Bahcall and J. Brinkmann, *Detection of massive tidal tails around the globular cluster Palomar 5 with Sloan Digital Sky Survey commissioning data*, The Astrophysical Journal **548** (2001), L165

[12] A. Bonaca and A.M. Price-Whelan, *Stellar streams in the Gaia era*, New Astronomy Reviews **100** (2025), 101713

[13] P.J. McMillan, *The mass distribution and gravitational potential of the Milky Way*, Monthly Notices of the Royal Astronomical Society **465** (2017), 76–94

Appendix A Some commonly used potentials

Kepler's point-mass potential is an oversimplified option for describing the potential of a star cluster. More realistic and widely used is the Plummer model for spherical systems. It assumes that the density of the system is roughly constant near the centre and falls to zero at large radii. The potential is then written as

$$\Phi = -\frac{GM}{\sqrt{r^2 + b^2}},$$

where b is the scale length and M is the total mass of the system [2].

Simple axisymmetric potentials frequently used for modelling Galactic potential are Kuzmin model and logarithmic potentials. Kuzmin model introduces potential of the form

$$\Phi = -\frac{GM}{\sqrt{R^2 + (a + |z|)^2}}, \qquad a \geq 0.$$

For points with $z < 0$ the potential is that of a point mass M located at $(R, z) = (0, a)$, while for $z > 0$ the potential corresponds to a point mass at $(0, -a)$. This potential is thus sometimes referred to as a razor-thin disk. A generalization of the model is called the Plummer-Kuzmin model, with potential

$$\Phi = -\frac{GM}{\sqrt{R^2 + (a + \sqrt{z^2 + b^2})^2}}, \qquad a, b = \text{const.}$$

When $a = 0$ the potential reduces to the Plummer model and when $b = 0$ the potential reduces to the Kuzmin model. Both of these models have circular velocities that fall off as $R^{-1/2}$ at large R. However, observed rotational curves of galaxies tend to be flat at large radii. To accommodate this we introduce the logarithmic potential

$$\Phi = \frac{1}{2} v_0^2 \ln \left(R_c^2 + R^2 + \frac{z^2}{q_\Phi^2} \right),$$

where R_c and v_0 are constants chosen such that the circular speed is consistent with observations and q_Φ is the axis ratio of equipotential surfaces [2].

In order to model more complex potentials, we usually combine multiple simple potentials, so that they represent different components of the Galaxy, such as the disk, bulge, bar, dark matter halo, etc [13].